Received: 13 August 2020 | Revised: 11 December 2020 | Accepted: 21 December 2020

DOI: 10.1096/fj.202001920RR

RESEARCH ARTICLE

THE FASEB JOURNAL

Phosphatase of regenerating liver-3 regulates cancer cell metabolism in multiple myeloma

Pegah Abdollahi[1,2] | Esten N. Vandsemb[1] | Samah Elsaadi[1] | Lisa M. Røst[3] | Rui Yang[1,2] | Magnus A. Hjort[1,4] | Trygve Andreassen[5] | Kristine Misund[1,6] | Tobias S. Slørdahl[1,6] | Torstein B. Rø[1,4] | Anne-Marit Sponaas[1] | Siver Moestue[1,7] | Per Bruheim[3] | Magne Børset[1,8]

[1]Department of Clinical and Molecular Medicine, Faculty of Medicine and Health Sciences, Norwegian University of Science and Technology, Trondheim, Norway

[2]Laboratory Clinic, St. Olavs University Hospital, Trondheim, Norway

[3]Department of Biotechnology and Food Science, Faculty of Natural Sciences, Norwegian University of Science and Technology, Trondheim, Norway

[4]Children's Clinic, St. Olavs University Hospital, Trondheim, Norway

[5]MR Core Facility, Department of Circulation and Medical Imaging, Faculty of Medicine and Health Sciences, Norwegian University of Science and Technology, Trondheim, Norway

[6]Clinic of Medicine, St. Olavs University Hospital, Trondheim, Norway

[7]Department of Pharmacy, Faculty of Health Sciences, Nord University, Bodø, Norway

[8]Department of Immunology and Transfusion Medicine, St. Olavs University Hospital, Trondheim, Norway

Abstract

Cancer cells often depend on microenvironment signals from molecules such as cytokines for proliferation and metabolic adaptations. PRL-3, a cytokine-induced oncogenic phosphatase, is highly expressed in multiple myeloma cells and associated with poor outcome in this cancer. We studied whether PRL-3 influences metabolism. Cells transduced to express PRL-3 had higher aerobic glycolytic rate, oxidative phosphorylation, and ATP production than the control cells. PRL-3 promoted glucose uptake and lactate excretion, enhanced the levels of proteins regulating glycolysis and enzymes in the serine/glycine synthesis pathway, a side branch of glycolysis. Moreover, mRNAs for these proteins correlated with PRL-3 expression in primary patient myeloma cells. *Glycine decarboxylase* (*GLDC*) was the most significantly induced metabolism gene. Forced GLDC downregulation partly counteracted PRL-3-induced aerobic glycolysis, indicating GLDC involvement in a PRL-3-driven Warburg effect. AMPK, HIF-1α, and c-Myc, important metabolic regulators in cancer cells, were not mediators of PRL-3's metabolic effects. A phosphatase-dead PRL-3 mutant, C104S, promoted many of the metabolic changes induced by wild-type PRL-3, arguing that important metabolic effects of PRL-3 are independent of its phosphatase activity. Through this study, PRL-3 emerges as one of the key mediators of metabolic adaptations in multiple myeloma.

Abbreviations: AMPK, AMP-activated protein kinase; B-ALL, B-cell acute lymphoblastic leukemia; CHAPS, 3-[(3-Cholamidopropyl)dimethylammonio]-1-propanesulfonate hydrate; DTT, Dithiothreitol; ECAR, extracellular acidification rate; ENO1, enolase 1; GLDC, glycine decarboxylase; GLUT1, Glucose transporter 1; GPI, glucose-6-phosphate isomerase; GSH, Glutathione; HIF-1α, hypoxia-inducible factor 1-alpha; HK2, hexokinase 2; IL-6, interleukin-6; LDHA, lactate dehydrogenase A; MCL-1, induced myeloid leukemia cell differentiation protein; MM, multiple myeloma; MTHFD, methylenetetrahydrofolate dehydrogenase; NMR, nuclear magnetic resonance; OCR, oxygen consumption rate; OXPHOS, oxidative phosphorylation; PBS, phosphate-buffered saline; PGAM1, phosphoglycerate mutase 1; PHGDH, phosphoglycerate dehydrogenase; PRL-3, phosphatase of regenerating liver-3; PSAT1, phosphoserine aminotransferase; PSPH, phosphoserine phosphatase; SHMT, hydroxymethyl transferase; SILAC, stable isotope labeling by amino acids in cell culture; TPI1, triosephosphate isomerase.

Pegah Abdollahi and Esten N. Vandsemb share first authorship to this article.

Correspondence
Magne Børset, Department of Clinical and Molecular Medicine, Norwegian University of Science and Technology, Trondheim 7491, Norway.
Email: magne.borset@ntnu.no

Funding information
NTNU; Liaison Committee for Education, Research, and Innovation in Central Norway

KEYWORDS
GLDC, glycine, PTP4A3, serine, Warburg effect

1 | INTRODUCTION

PRL-3, a phosphatase encoded by the gene *PTP4A3*, is ectopically expressed in many cancers, particularly in metastatic tumors.[1] This was first observed in several carcinomas,[2-6] and later in hematopoietic cancers like multiple myeloma (MM), leukemia, and lymphoma.[7-13] PRL-3 is regulating magnesium homeostasis[14-17] and a series of cell signaling events.[18]

MM, the cancer of plasma cells, occurs mainly in the bone marrow. Despite several new treatment options in recent years, it is still considered an incurable disease. MM cells are dependent on signals from the microenvironment, and the cytokine interleukin (IL)-6 is one of the molecules allowing them to survive and proliferate.[19,20] Growth factor signals are critical not only for cell proliferation, but also for import and processing of nutrients.[21] Metabolic adaptations are not merely an intrinsic response to the proliferative stimulus but also regulated by external signals that can be separated from the proliferative signal.[22]

PRL-3 is highly expressed in MM cells in a large proportion of patients[7] and correlates strongly with an unfavorable prognosis for patients with MM.[23,24] We have previously shown that PRL-3 is induced in MM cells by growth factors such as IL-6,[7,25] and that PRL-3 protects cells against apoptosis without contributing to proliferation. This is mediated by the oncoprotein Src and stabilization of the anti-apoptotic protein MCL-1.[25,26] As there is a complex interplay between metabolism, proliferation, and cell death, we wanted to examine whether PRL-3 regulates the metabolic adaptation of cancer cells.

2 | MATERIALS AND METHODS

2.1 | Cell culture

All cells were grown in RPMI-1640 supplemented with 0.68 mM of L-glutamine and 10%-20% heat-inactivated fetal calf serum (FCS). INA-6 was cultured in media with 1 ng/mL of IL-6. Cells were cultured at 37°C in a humidified atmosphere with 5% CO_2 and growth media were replenished twice weekly. Human myeloma cell lines INA-6 and JJN-3 were a gift from Dr. M. Gramatzki, University of Erlangen-Nurnberg, Germany and Dr. I.M. Franklin, University of Birmingham, UK, respectively. Human Hodgkin's lymphoma cell line L1236 (ACC 530) was from DSMZ (Brauschweig, Germany) and human B-ALL cell line Reh from ATCC (Rockville, MD). Cells were cultured as described previously.[8,9,25] New cultures of cells were seeded at least every 4 months from vials aliquoted with cells propagated shortly after receiving the cells from their described original source, and they were regularly tested to ensure absence of mycoplasma. For hypoxic conditions cells were kept in an incubator with 2% O_2. In order to deplete cells of IL-6 before experiments, they were washed three times with Hanks' balanced salt solution (HBSS) (Sigma-Aldrich, St. Louis, MO). When glucose starvation was performed, cells were grown in glucose-free RPMI-1640 Medium (Thermo Fisher Scientific, MA) and in conditions where serine and/or glycine were depleted, MEM medium (Cat No#21090022, Thermo Fisher Scientific) was used.

2.2 | Antibodies, cytokines, and other reagents

IL-6 was from Biosource (Camarillo, CA). PRL-3 inhibitor I (5-[[5-Bromo-2-[(2-bromophenyl)methoxy]phenyl] methylene]-2-thioxo-4-thiazolidinone) was from Sigma-Aldrich. Thienopyridone was a gift from Professor John S. Lazo (University of Virginia, Charlottesville, VA). Serine (S4500) and glycine (104201) were purchased from Sigma-Aldrich and Millipore, respectively.

PBMN-ires-GFP was a gift from Garry Nolan (Addgene 130 plasmid # 1736), pLKO and shRNA-pLKO against PRL-3 were a gift from Dr. Jim Lambert (University of Colorado, Denver, CO). pLenti CMV Puro DEST (w118-1) was a gift from Eric Campeau & Paul Kaufman (Addgene plasmid # 17452).[27]

Antibodies against β-Tubulin (#2146), hexokinase II (#2867), GLUT1 (#12939), SHMT2 (#12762), PHGDH (#66350), β-actin (#4967), MTHFD2 (#41377), Phospho-AMPKα (Thr172) (#2535), LDHA (#3582), c-Myc

(#5605), PGAM1 (#12098), Aldolase A (#8060), and AMPKα (#5832) were purchased from Cell Signaling Technology (BioNordika AS, Oslo, Norway). Antibodies against CD98 (#sc-376815), PRL-3 (318) (#sc-130355), GLDC (#sc-376196), and PSPH (#sc-271421) were purchased from Santa Cruz Biotechnology (Dallas, TX). Antibodies against HIF-1 alpha (#AF1935), PSAT1 (#PA5-22124), GCAT [EPR13450]—N-terminal (#ab181094), and GPI (#HPA024305) were purchased from R&D systems (Minneapolis, MN), Invitrogen (Waltham, MA), Abcam (Cambridge, UK) and Sigma-Aldrich, respectively. All siRNAs used were ON-TARGETplus siRNAs from Dharmacon (Lafayette, CO) : against GLDC (J-009305-06-0002, J-009305-07-0002, J-009305-08-0002, J-009305-09-0002, LU-009305-00-0002), against AMPKα1 (J-005027-06-0002, J-005027-06-0002, against AMPKα2 (J-005361-07-0002, J-005361-06-0002), and control siRNA (D-001810-10-05).

2.3 | Viral transduction

PRL-3 in JJN-3 cells was expressed by lentiviral transduction as described previously.[8,9] pLenti CMV Puro DEST-PTP4A3 or pLenti CMV Puro DEST (Control plasmid) was used to establish PRL-3-JJN-3 and Mock-JJN-3. Transduced cells were grown in medium containing 0.2 μg/ml of puromycin for selection. PRL-3 in L1236 and Reh cells was stably knocked down by lentiviral transduction as described previously.[8,9]

PRL-3 was overexpressed in INA-6 by retroviral transduction as previously described.[26] Cells were cloned by limiting dilution to yield individual clones followed by the analysis of PRL-3 protein levels.

2.4 | Nucleofection

Gene knockdown by siRNA was performed as described previously[25] using Amaxa Cell Line Nucleofector Kit R, [Lonza, Switzerland]). Briefly, cells in transfection buffer were added to separate nucleofection cuvettes containing 1 μM of four individual siRNAs and transfected by a Nucleofector II device (Lonza) (program X-001 and T-001 were used for INA-6 and JJN3, respectively).

2.5 | Immunoblotting

Cells were treated as indicated and collected, lysed and immunoblotting was performed as described previously.[25] Images were acquired using LI-COR Odyssey Fc and analyzed with Image Studio Software (LI-COR, Lincoln, NE).

2.6 | Relative ATP measurement

Level of cellular ATP production was estimated using CTG Cell Viability Assay (Promega, Fitchburg, WI) as described previously.[26]

2.7 | Cell viability

Apoptosis was evaluated using Annexin V-Alexa Fluor 647 binding (A23204, Thermo Fisher, MA), as previously described.[25]

2.8 | Glutathione (GSH) levels

GSH levels were measured using the GSH-GLO Assay (Promega) according to the manufacturer's instructions. Briefly, 20 000 cells were seeded in 25 μL of PBS per well. Reagents were added according to the protocol from Promega, and the luminescent signal was detected by Victor3 plate reader (PerkinElmer, CT) with Wallac 1420 Work Station software.

2.9 | Glycolytic flux

Glycolysis and oxidative phosphorylation (OXPHOS) in cells were measured using Glycolysis stress and Cell Mito Stress test kits in Seahorse XF96 bioanalyzer (Seahorse Bioscience, North Billerica, MA) according to the manufacturer's instructions. Briefly, 96-well Seahorse cell culture plates were coated with cell-tak in advance and 25 000 viable cells were cultured per well on day of experiment. To hydrate a sensor cartridge, 200 μL of distilled sterile water was added to each well of the XF Utility Plate. The XF Sensor Cartridge was placed on top of the utility plate and incubated overnight in 37°C without CO_2. 45-60 minutes before experiment, water was replaced with Seahorse Calibrant solution. On the day of experiment, assay medium was prepared by supplementing Seahorse XF Base Medium (102353-100, Seahorse Bioscience) with 2 mM of glutamine, warming it up to 37°C and setting the pH to 7.4 with 0.1 N NaOH. A total of 25 000 cells/50 μL of assay media was seeded per well and incubated for approximately 30 minutes in 37°C incubator without CO_2 to ensure that the cells had completely attached. A total of 130 μL of warm assay medium was added gently along the side of each well to get the final volume of 180 μL.

We used the constant compound concentration with variable loading volume approach.

For Glycolysis Stress test, glucose (G7021, Sigma-Aldrich), oligomycin (O4876, Sigma-Aldrich), and

2-deoxy-D-glucose (D8375, Sigma-Aldrich) were loaded into ports A, B, and C of a hydrated sensor cartridge. Final concentration used for glucose, oligomycin, and 2-deoxy-D-glyucose was 10 mM, 1 μM, and 50 μM, respectively.

For the Cell Mito Stress test kit the Seahorse XF Base Medium was supplemented with 2 mM of glutamine, 10 mM of Na-Pyruvate (p5280, Sigma-Aldrich) and glucose. Ports A, B, and C were loaded with oligomycin, FCCP (C2920, Sigma-Aldrich), and Antimycin/Rotenone (A8674 and R8875, Sigma-Aldrich), respectively. Final concentration used was 1 μM of oligomycin and FCCP and 2 μM of Antimycin/Rotenone.

For measuring glycolysis and OXPHOS a program with 2-minute mixture, followed by 5-minute measurement after each injection was used. Data were analyzed using Agilent Seahorse Analyzers Wave 2.6.

2.10 | Quantification of extracellular glucose, glutamine, and lactate

Four parallel cultures of PRL-3-INA-6, PRL-3-JJN-3, and mock cells were seeded at a density of 4-7 × 10^5 cells/mL with (INA-6) and without (INA-6 and JJN-3) IL-6 and incubated for 24 hours. Fresh and conditioned medium samples were collected and processed for the quantification of extracellular levels of glucose, glutamine, and lactate by nuclear magnetic resonance (NMR) as described previously.[28] Consumption and production over 24 hours were normalized to average number of live cells in the 24-hour interval to obtain consumption/production /cell/24 hours.

2.11 | Analysis of CoMMpass data

RNA-seq data on purified MM cells from 767 patient samples were downloaded from the CoMMpass (IA12 release) and used for gene expression analysis. The patient samples were divided into two different groups based on PRL-3 expression: 50% High PRL-3 expression vs 50% low PRL-3 expression. Reactome pathway analysis was performed on differentially expressed genes between the two groups in the Multiple Myeloma Research Foundation research gateway.

2.12 | SILAC-based Quantitative Mass Spectrometry

We first cultured cells in Pierce SILAC Protein Quantitation Kit—RPMI-1640 (Thermo Fisher). RPMI without L-Lysine or L-Arginine was supplemented with 0.68 mM of L-glutamine, 40 μg/mL of gentamicin, 10% dialyzed fetal bovine serum, and either 100 μg/mL (L-Lysine-2HCl and L-Arginine-HCl) or ($^{13}C_6$ L-Lysine-2HCl and L-Arginine-HCl) to create SILAC-"Light" or SILAC-"Heavy" medium, respectively. Two different clones of PRL-3-INA-6 (clone 1 and clone 2) and two different clones of mock control (clone 1 and clone 2) counterparts were grown in both SILAC-Heavy and SILAC-Light medium, for a total of seven passages before testing the labeling efficiency of the SILAC-Heavy medium.

Cells were depleted of IL-6 as described above and starved for 12 hours in the absence of IL-6. An equal number of heavy and light (5 × 10^5 each) cells were collected and lysed in 7 M of urea, 2 M of thiourea, 2.5% of (w/v) CHAPS, and 25 mM of DTT for 30 minutes with shaking. Lysates were clarified by centrifugation at 16 000 *g* for 15 minutes and proteins in the soluble fractions were precipitated using chloroform/methanol as described previously.[29] Briefly, 100 μL of lysate was mixed with 400 μL of methanol, 100 μL of chloroform, and 300 μL of water sequentially. The mixture was then centrifuged for 2 minutes at 16 000 *g*. The upper layer was discarded and 400 μL of methanol was added to the pellet and centrifuged for 2 minutes at 16 000 *g*. The pellet was re-suspended in 150 μL of 50 mM NH_4HCO_3. To reduce disulfide bonds, 7.5 μL of 200 mM DTT was added and the mixture was incubated at 70°C for 20 minutes. The reduced cysteines were alkylated adding 30 μL of 200 mM iodoacetamide and further incubated at room temperature in the dark for 30 minutes. Finally, digestion was done at 37°C overnight with gentle shaking by adding 1.25 μg of trypsin. The peptides were dried down using SpeedVac before fractionation using strong anion exchange combined with C-18 reversed phase, SAX in StageTip format and using three different pHs, pH-11, pH-6, and pH-3 as described previously.[30] After desalting, the peptides were dried in a SpeedVac centrifuge and resuspended in 0.1% formic acid.

The peptides were analyzed on a LC-MS/MS platform consisting of an Easy-nLC 1000 UHPLC system (Thermo Scientific/Proxeon) interfaced with an LTQ-Orbitrap Elite hybrid mass spectrometer (Thermo Scientific) via a nanospray ESI ion source (Proxeon, Odense, Denmark). Peptides were injected onto a C-18 trap column (Acclaim PepMap100, 75 μm i. d. × 2 cm, C18, 5 μm, 100 Å, Thermo Scientific) and further separated on a C-18 analytical column (Acclaim PepMap100, 75 μm i. d. × 50 cm, C18, 3 μm, 100 Å, Thermo Scientific) using a 270-min multistep gradient with buffers A: 0.1% formic acid and B: CH_3CN, 0.1% formic acid at a flow rate of 250 nL/min. 0-252 minutes 0%-30% B, 252-257 minutes 30%-100% B, 257-262 minutes 100% B, 262-263 minutes 100%-0% B, and finally 0% B for 7 minutes. Peptides eluted were analyzed on the LTQ-Orbitrap Elite hybrid mass spectrometer operating in positive ion- and data-dependent acquisition (DDA) mode using the following parameters: Electrospray voltage 1.9 kV, CID fragmentation

with normalized collision energy 35, automatic gain control (AGC) target value of 1E6 for Orbitrap MS, and 1E3 for MS/MS scans. Each MS scan (m/z 400-1600) was acquired at a resolution of 120 000 FWHM, followed by 20 MS/MS scans triggered for intensities above 500, at a maximum ion injection time of 200 ms for MS and 50 ms for MS/MS scans.

The raw data files were analyzed using Proteome Discoverer Software (Thermo Fisher) mapping the spectra over Human proteome downloaded from UniProt.[31] Search parameters used were as follows: enzyme specified as Trypsin with maximum two missed cleavages allowed; Heavy Lysine ^{13}C (6) + 6.020 Da as variable modification; maximum allowed delta Cn of 0.05; and precursor mass tolerance was set to 10 PPM with fragment mass tolerance of 0.6 Da. Percolator[32] was used to control false discovery rate (FDR) for spectra identification and FDR was set to <0.01 (high confidence) for selecting peptides used for inferring proteins. Median values of uniquely mapped peptide were used for calculating SILAC ratio for each protein.[33] These ratios were log transformed with base 2 (log2). IDs detected in at least two out of three biological replicates were kept for further analysis. One sided Student's *t* test was performed for individual time point and *P*-values were corrected with Benjamini and Hochberg algorithm[34] using Perseus platform.[35]

2.13 | ^{13}C NMR of cell extracts

PRL-3-INA-6 and Mock-INA-6 were incubated at 0.8×10^6 cells/mL for 6 hours in a modified DMEM solution (D9802-01, US biologicals) containing 2.0 g/L of D-Glucose-1,2-$^{13}C_2$ (453188, Sigma-Aldrich, USA), 2.0 g/L of sodium bicarbonate, 2.7 mM of glutamine, and 10% heat-inactivated dialyzed FBS (Gibco), and without serine and glycine. Approximately 4×10^7 cells were washed with 50 mL of PBS and spun to a pellet (1500 RPM, 8 min) two times. Extraction with 10 mL of ice-cold (−20°C) 80:20 methanol/water was performed twice. The extracts were vacuum-dried for 20 hours and stored at −80°C, before reconstitution in 600 μL of D_2O and transfer to 5 mm NMR tubes. NMR analysis was performed using a 600 MHz Bruker Avance III NMR spectrometer (Bruker Biospin GmbH, Germany), equipped with a 5 mm QCI Cryoprobe with integrated, cooled preamplifiers for ^1H, ^2H, and ^{13}C. Proton spectra were acquired at 300 K using 1D NOESY (Bruker: noesygppr1d) with presaturation and spoiler gradients as previously described.[36] The spectra were collected with 128 scans and 4 dummy scans. The acquisition time was 2.73 s and relaxation delay 4 s, measuring the free induction decay (FID) via collection of 64 K complex data points. Proton decoupled ^{13}C spectra (Bruker: zgpg30) were acquired using a power gated coupling sequence with a 30º pulse angle as described in Bettum et al.[37] The spectra were collected with 16 K scans and 16 dummy scans. The acquisition time was 1.65 s, relaxation delay 0.5 s, measuring the FID via collection of 96 K complex data points over a sweep width of 197.175 ppm. The ^{13}C spectra were Fourier-transformed with a 3.0 Hz exponential line broadening and the chemical shift was calibrated to the residual methanol signal at 51.4 ppm. Levels of selected metabolites in the extracts were semiquantitatively assessed by the integration of resonance signals using TopSpin 4.0.8 (Bruker Biospin).

2.14 | Statistical analysis

Two-tailed Student's *t* test or Mann-Whitney U test was used for normally distributed and non-normally distributed data, respectively. Correlation coefficients were determined with Spearman correlation analysis. The Kaplan-Meier method was used for survival analyses, and the survival curves were compared with the log-rank test. The statistical analyses were performed in GraphPad Prism (version 5.03 or 7.0).

3 | RESULTS

3.1 | PRL-3 is highly expressed in myeloma cells

The IL-6 target PRL-3 protects MM cells against apoptosis but does not stimulate proliferation.[7] Additional support for the importance of PRL-3 in MM was found in gene array mRNA data from 917 different cell lines in the Cancer Cell Line Encyclopedia[38] deposited in the database Oncomine (Figure 1A). MM cell lines (n = 26) had on average higher expression of the PRL-3 gene (*PTP4A3*) than all other cancer entities. The only comparable entity was leukemia, suggesting that the expression of PRL-3 is of particular importance for several cancers of hematopoietic origin.

3.2 | PRL-3 promotes cell growth and ATP production but not proliferation

We transduced INA-6 and JJN-3 myeloma cells with an empty control vector (Mock-INA-6 and Mock-JJN-3) or an expression vector encoding wild-type (WT) PRL-3 (PRL-3-INA-6 and PRL-3-JJN-3) or mutated enzyme-inactive PRL-3 (C104S-INA-6 and C104S-JJN-3). As in our previous studies of PRL-3 in MM[7,25] PRL-3 protected against apoptosis without regulating proliferation (Figure 1B). However, cells overexpressing PRL-3 had larger cell diameter than mock cells (Figure 1C) indicating that PRL-3 causes cell growth without stimulating proliferation.

Cells overexpressing PRL-3 also had higher ATP level than mock cells (Figure 1D,E). The PRL-3 inhibitor

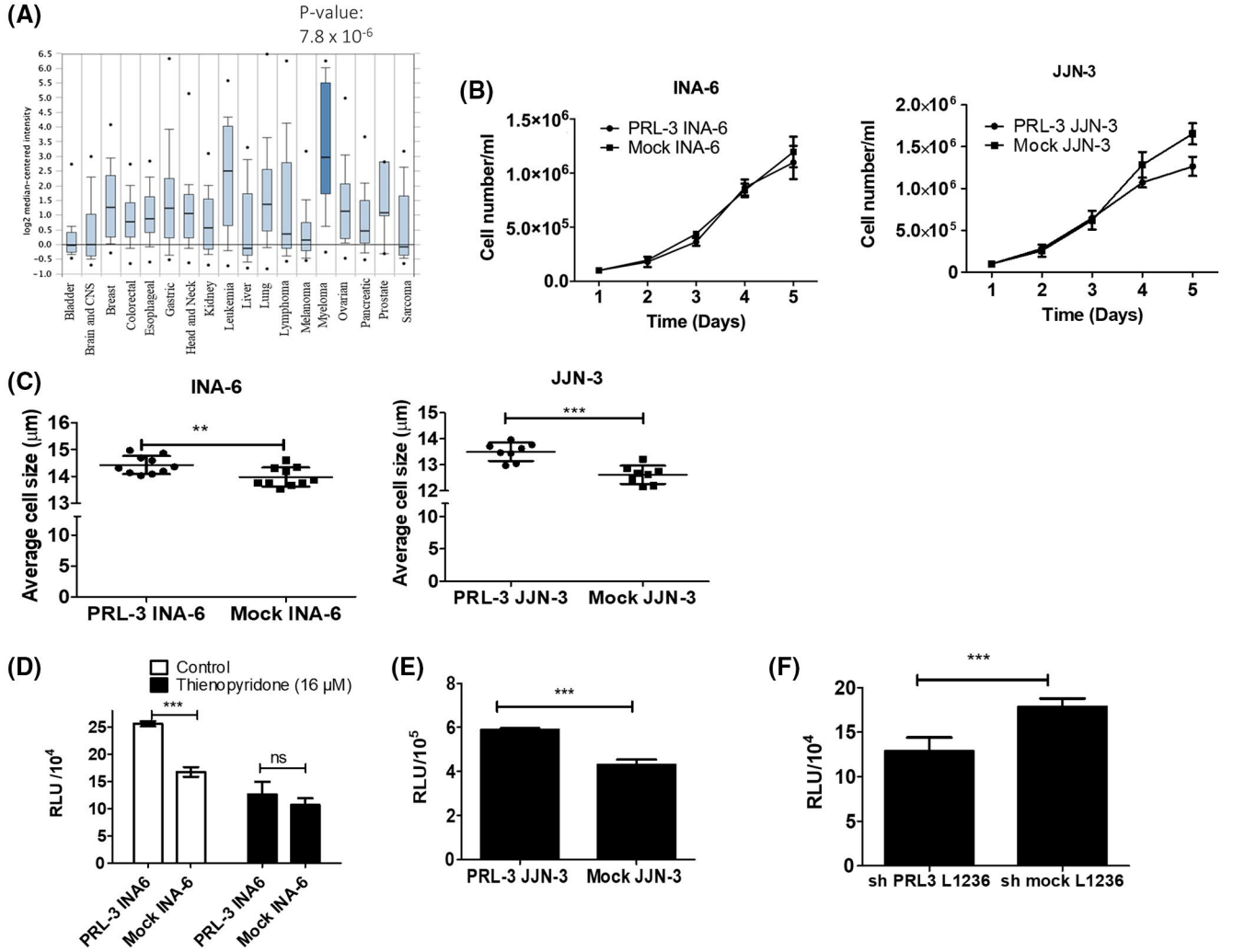

FIGURE 1 PRL-3 enhances cell growth and ATP production. A, Expression of PRL-3 mRNA in cell lines from 18 different cancer entities in Barretina datasets derived from the public database Oncomine. *P*-value refers to a *t* test of the difference between expression in MM cells (n = 26) and in all other entities combined (n = 891). B, Proliferation was measured in INA-6 and JJN-3 cells using Coulter counter. Plots show mean of two independent experiments, each with two replicates. C, Cell diameter was measured in INA-6 and JJN-3 cells using Coulter counter. ATP levels measured by the Cell Titer-Glo assay after lysing an identical number of cells in (D) PRL-3 INA-6 and mock cells grown with or without PRL-3 inhibitor thienopyridone for 4 days, (E) PRL-3 JJN-3 and control mock cells, and (F) shPRL-3 L1236 cells and mock control cells. Plot D shows one representative out of two independent experiments, each with five replicates, plot E shows mean of two independent experiments with three replicates each, and plot F shows the mean of three independent experiments with minimum four replicates each. Error bars show ± SD. ns, not significant, $^{**}P \leq .01$, $^{***}P \leq .001$.

thienopyridone, at a concentration that was not inhibitory to cell viability (Figure S1A), reduced ATP production in PRL-3-INA-6 to the level in Mock-INA-6 (Figure 1D). Finally, Hodgkin lymphoma cell line L1236 with stable PRL-3 knockdown had lower ATP content than L1236 mock cells (Figure 1F).

3.3 | PRL-3 increases glycolytic flux and oxidative phosphorylation

Since OXPHOS and glycolysis are the major sources of ATP, we measured the activity in these metabolic pathways. Glycolysis was measured by extracellular acidification rate (ECAR) with a Seahorse XF analyzer. ECAR largely reflects the extracellular lactate concentration, which in turn is determined by the rate of glycolysis. PRL-3-INA-6 and PRL-3-JJN-3 showed higher glycolytic rate than their respective mock cells (Figure 2A). The transduction of INA-6 cells to express PRL-3 was repeated, and two individual pairs of clones (PRL-3 and MOCK) from this transduction were examined and showed identical results to those in Figure 2A (data not shown). Both transient knockdown of endogenous PRL-3 and thienopyridone treatment caused a significant reduction in glycolytic rate (Figure 2B,C). However, 8 and 16 μM of thienopyridone

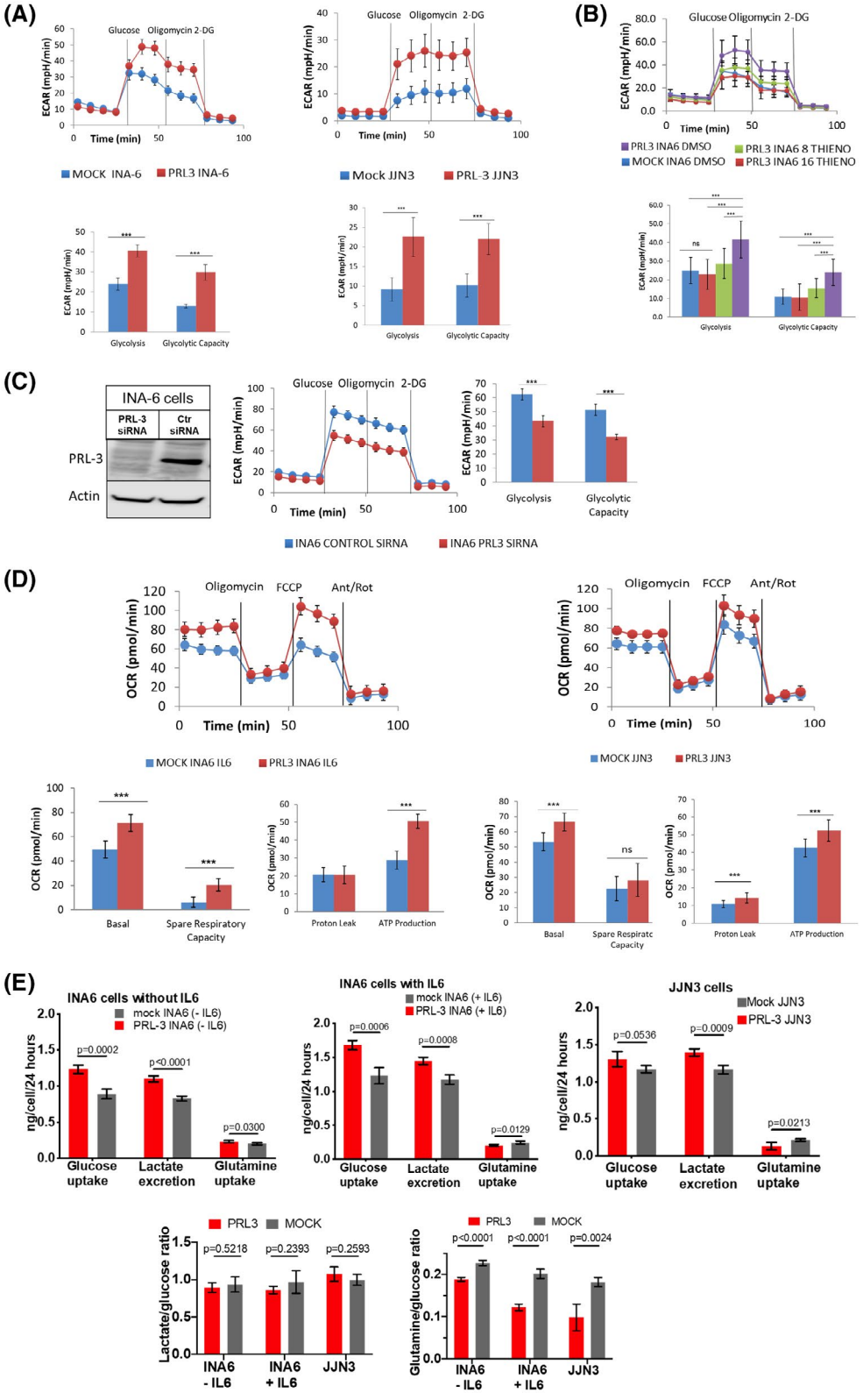

FIGURE 2 PRL-3 increases glycolysis flux and oxidative phosphorylation. Glycolysis parameters (glycolysis and glycolysis capacity) and Oxidative phosphorylation parameters (basal respiration, spare respiratory capacity, proton leak, and ATP production) were measured by a Seahorse XF analyzer. Glycolysis in (A) PRL-3-INA-6, PRL-3-JJN-3, and their control mock cells. B, PRL-3-INA-6 and mock cells treated with the PRL-3 inhibitor thienopyridone (8 and 16 μM) or DMSO for 24 h before glycolysis measurements. C, Glycolysis in INA-6 cells after transient knockdown of PRL-3 by siRNA. Knockdown efficacy is shown by WB. D, Oxidative phosphorylation in PRL-3-INA-6, PRL-3-JJN-3 MM cells, and their respective mock cells. INA-6 were grown with IL-6. Seahorse graphs show one representative out of at least two independent experiments, each with 24 technical replicates. E, Average glucose and glutamine consumption and lactate excretion as well as, lactate/glucose and glutamine/glucose ratios were quantified by NMR. Measurements were done in PRL-3-INA-6 and mock cells with and without IL-6, and in PRL-3-JJN-3 and mock without IL-6. Error bars show ± SD. ns, not significant, $***P \leq .001$

(A)

		SILAC-proteomics PRL-3 vs. Mock	
Cell line		INA-6	
IL-6 starvation?		Yes, 12h	
		Log2 fold change	p value
HK1	Enzymes involved in glycolysis	ND	ND
HK2		1.09	0.0007
GPI		1.14	0.002
PFKP		ND	ND
PFKM		ND	ND
PFKL		ND	ND
PFKFB3		ND	ND
PFKFB4		ND	ND
ALDOA		1.06	0.005
TPI1		0.95	0.001
GPDH		ND	ND
PGK1		ND	ND
PGAM1		0.90	0.02
ENO1		0.99	0.0001
PKM2		ND	ND
LDHA		1.14	0.0004
SLC2A1	Transporter molecules	1.66	0.06
SLC2A3		ND	ND
SLC2A5		ND	ND
SLC1A5		1.62	0.0006
SLC3A2		2.70	0.007
SLC7A5		2.04	0.001
GLDC	Enzymes involved in serine/glycine pathway	2.81	0.02
SHMT2		0.64	0.0003
SHMT1		ND	ND
GCAT		ND	ND
PHGDH		0.52	0.0008
PSAT1		ND	ND
PSPH		1.03	0.001
MTHFD1		ND	ND
MTHFD2		1.21	0.002
ATF4	Proteins regulating metabolism	ND	ND
C-MYC		ND	ND
HIF1α		ND	ND
AMPKα1		ND	ND
AMPKα2		ND	ND

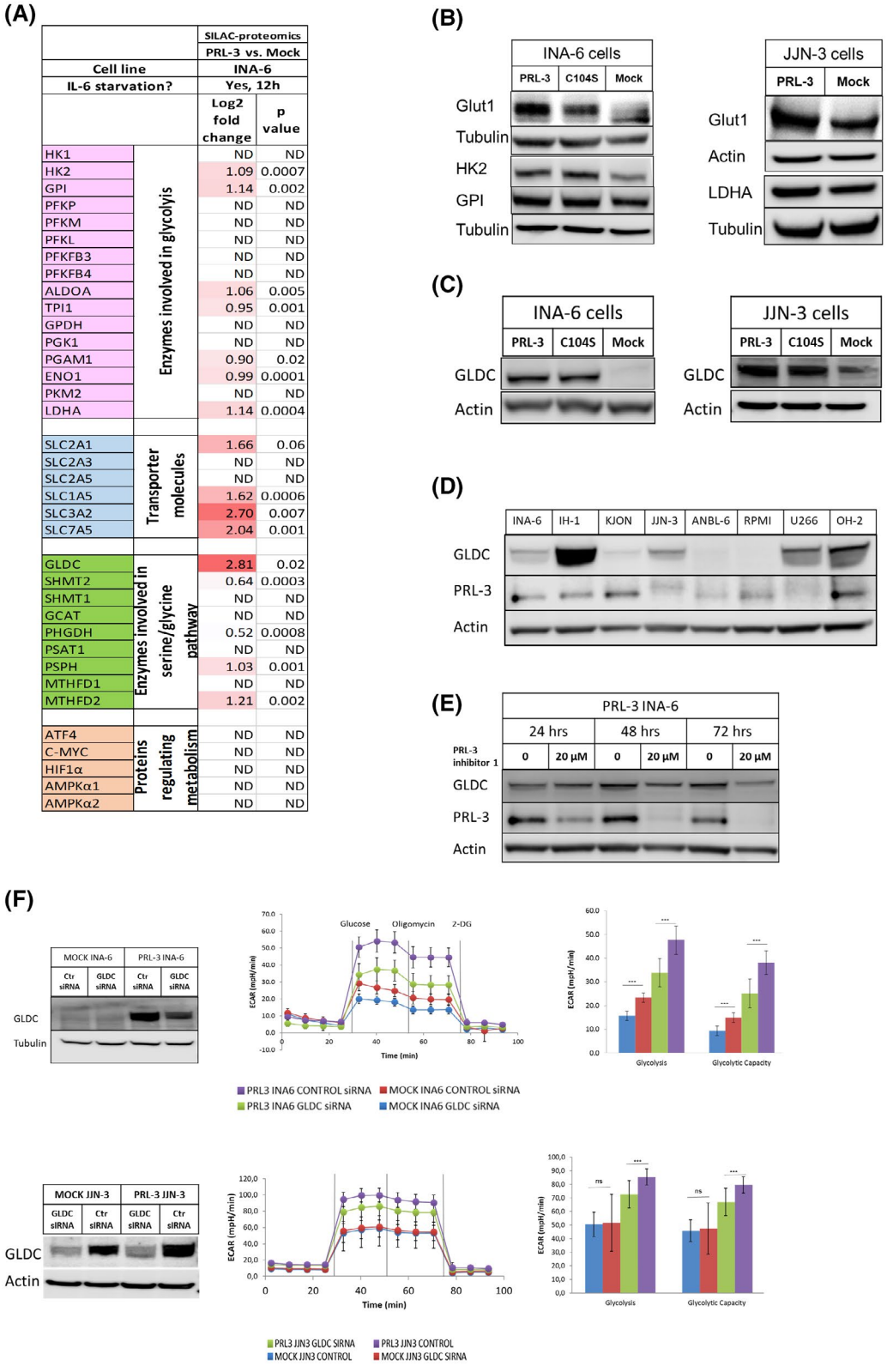

FIGURE 3 PRL-3 regulates glycolysis through upregulation of glycolytic enzymes and GLDC. A, Expression levels of selected proteins involved in metabolome regulation in PRL-3-INA-6. Dark red and light red indicate higher and lower log2 fold change values, respectively. ND, not detected. INA-6 and JJN-3 cells overexpressing wild type (WT) or catalytically dead mutant (C104S) PRL-3, and mock control cells were immunoblotted with (B) indicated antibodies and (C) anti-GLDC. INA-6 cells were starved of IL-6 before cell harvest to reduce endogenous levels of PRL-3. D, Various MM cell lines were immunoblotted with anti-GLDC and anti-PRL-3. E, PRL-3 INA-6 cells were treated with PRL-3 inhibitor 1 for indicated time periods and immunoblotted with anti-GLDC and anti-PRL-3. F, GLDC was knocked down in PRL-3-INA-6/JJN-3 and their control mock cells by transient transfection. Glycolysis was measured 48 h after nucleofection. Protein lysates were prepared from the same cells and GLDC protein level was measured by Western blot (left panel). Seahorse graphs are one representative out of at least two independent experiments, each with 24 technical replicates. Error bars show ± SD. ns, not significant, ***$P \leq .001$

caused 8.8% and 22.3% reduction in cell viability relative to the control, respectively (Figure S1B). Still, the magnitude of the change in glycolysis is larger than the change in viability. We measured oxygen consumption rate (OCR) with the Seahorse XF Cell Mito Stress Test. PRL-3-expressing INA-6 and JJN-3 cells had a higher level of basal respiration as well as ATP production than mock cells. Spare respiratory capacity was only higher in PRL-3-INA-6 cells than in mock cells (Figure 2D).

To see if PRL-3 regulated glycolysis in other hematopoietic cancers, we measured ECAR in L1236 and the B-ALL cell line Reh. In cells with stable knockdown of PRL-3,[8,9] glycolysis, and glycolytic capacity were lower in Reh cells (Figure S2A) and glycolytic capacity was lower in L1236 cells (Figure S2B) than in the respective mock cells.

3.4 | PRL-3 promotes glucose import and lactate export

NMR-based quantification of the main carbon sources (glucose and glutamine) and excretion products in conditioned media revealed significantly higher lactate excretion from PRL-3-INA-6 and PRL-3-JJN-3 cells than from mock cells (Figure 2E), confirming the increased ECAR in Seahorse experiments. The high lactate excretion rate was accompanied by increased glucose uptake in both PRL-3-JJN-3 and -INA-6, leaving the lactate/glucose ratio equal in PRL-3 and mock cells (Figure 2E). The higher consumption of glucose combined with higher excretion of lactate suggested an overall higher glycolytic flux induced by PRL-3. Notably, PRL-3 also affected the balance between uptake of glucose and glutamine. The glutamine/glucose ratio was significantly lower in PRL-3-INA-6 and PRL-3-JJN-3 cells than in mock cells (Figure 2E), indicating that PRL-3 overexpression shifts the energy and carbon source preference to glucose at the expense of glutamine.

3.5 | PRL-3 influences protein expression of molecules regulating metabolism

We performed proteome profiling of INA-6 cells with SILAC-based quantitative mass spectrometry. In order to eliminate the role of IL-6-induced PRL-3, we cultured INA-6 cells in the absence of IL-6 for 12 h. Figure 3A shows molecules that are central to cellular metabolism. Here, we observed the upregulation of many enzymes that catalyze the glycolytic pathway.

The most conspicuous result of forced PRL-3 expression was a marked upregulation of glycine decarboxylase (GLDC) protein. Synthesis of serine and further glycine is one of the side branches of glycolysis. GLDC decarboxylates glycine, thereby transferring carbon into the folate-mediated one-carbon metabolism and providing one-carbon units for the production of nucleotides and other biomolecules.

In addition, GLDC is a potent regulator of glycolysis.[39-42] We also noticed that transporter molecules and enzymes regulating amino acid metabolism (serine/glycine synthesis pathway) were influenced by PRL-3 expression.

3.6 | PRL-3-driven glycolysis is influenced by glycolytic enzymes and GLDC, but not by AMPK, HIF-1α, and c-Myc

The glucose transporter GLUT1 (gene name: *SLC2A1*), was upregulated by PRL-3 in the proteomics analysis (Figure 3A) and by Western blotting (WB) in both INA-6 and JJN-3 (Figure 3B). In INA-6 cells, there was not only an increased total amount of GLUT1 in PRL-3 cells, but also a gel mobility shift, possibly due to the posttranslational modifications of GLUT1.

Enzymes catalyzing glycolysis, hexokinase 2 (HK2), glucose-6-phosphate isomerase (GPI), aldolase, triosephosphate isomerase (TPI1), phosphoglycerate mutase 1 (PGAM1), enolase 1 (ENO1), and lactate dehydrogenase A (LDHA), were all found in close to double protein concentrations in PRL-3-INA-6 compared to Mock-INA-6 (Figure 3A). But of those tested, only HK2 and GPI in INA-6, and LDHA in JJN3 were detected at a clearly higher protein level by WB (Figure 3B and Figures S3 and S4).

Since GLDC was the enzyme most significantly upregulated by PRL-3 (Figure 3A,C), we wanted to see whether it was a mediator of metabolic responses to PRL-3. Publicly available data from the Cancer Cell Line Encyclopedia[38] show high expression of GLDC in myeloma cells (Figure S5). We detected GLDC protein expression in six out of eight MM cell lines, but without clear correlation with PRL-3 expression (Figure 3D). To confirm that PRL-3 was crucial for the upregulation of GLDC, we treated INA-6 cells with PRL-3 inhibitor 1, which leads to PRL-3 degradation. After 72 hours, PRL-3 was downregulated and GLDC level decreased (Figure 3E). However, we could not exclude the possibility that PRL-3 inhibitor I might have off-target effects toward other PRL members. Transient knockdown of GLDC reduced glycolysis in both PRL-3-INA-6, Mock-INA-6, and in PRL-3-JJN3, identifying GLDC as another mediator of high glycolysis by PRL-3 (Figure 3F).

AMP-activated protein kinase (AMPK), HIF-1α, and c-Myc are important regulators of glycolysis.[43] Neither c-Myc nor HIF-1α contributed to PRL-3-driven glycolysis in INA-6 cells (Figure 4A,C). Conversely, there was no increase in PRL-3 protein levels in Mock-INA-6 cells cultured in hypoxia (Figure 4A). Preincubating cells in hypoxia promoted glycolysis in INA-6 cells and weakly in PRL-3-JJN-3 cells.

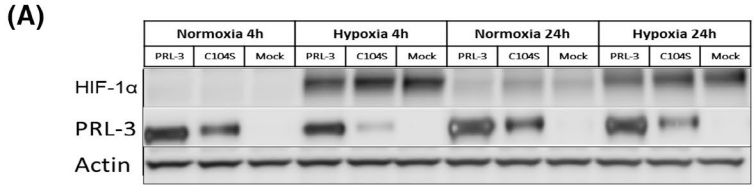

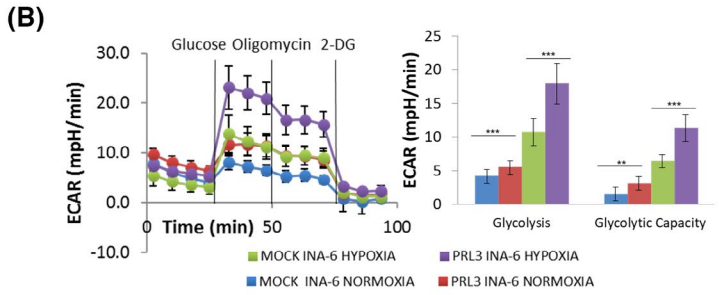

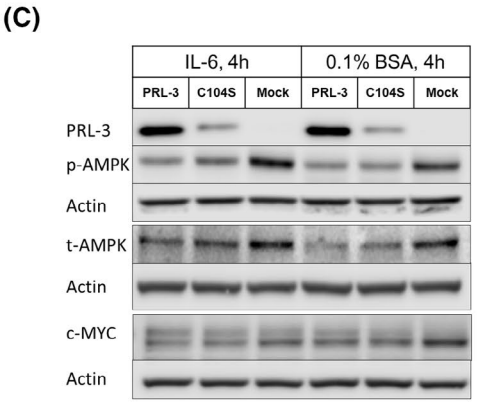

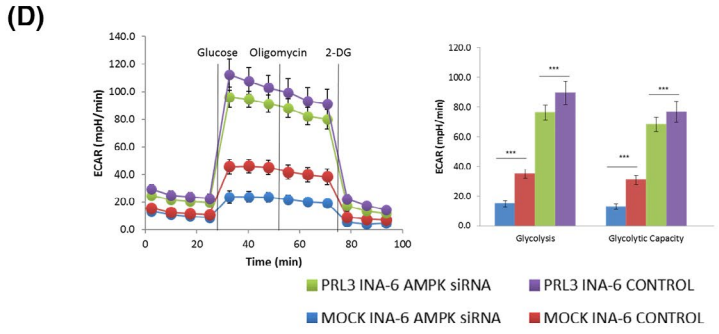

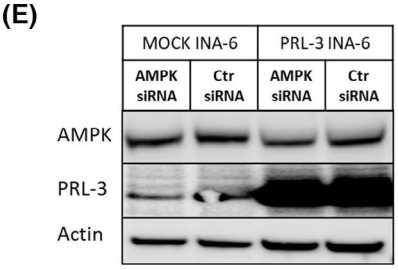

(F)

	PTP4A3	HK1	HK2	GPI	PFKP	PFKM	PFKL	PFKFB3	ALDOA	TPI1	GAPDH	PGK1	PGAM1	ENO1	PKM2	LDHA	c-Myc	HIF1α	AMPKα1	AMPKα2
PTP4A3		0,17	0,12	0,19	0,11	0,12	-0,05	-0,17	0,16	0,17	0,25	0,31	0,22	0,07	-0,04	0,36	0,03	0,14	-0,12	0,14
HK1	1E-06		0,15	0,21	0,22	0,06	-0,04	0,16	0,17	0,05	0,25	0,17	0,20	0,06	0,19	0,17	0,09	0,17	0,06	-0,02
HK2	0,001	3E-05		0,40	0,09	0,32	-0,06	-0,01	-0,02	0,25	0,24	0,15	0,09	0,34	0,31	0,30	0,37	0,22	0,08	-0,05
GPI	2E-07	3E-09	4E-31		-0,17	0,50	-0,12	-0,22	0,28	0,46	0,45	0,30	0,35	0,38	0,44	0,38	0,26	-0,03	0,22	-0,16
PFKP	0,002	1E-09	0,01	3E-06		-0,16	0,13	0,19	0,20	0,01	0,04	0,11	0,01	0,05	0,05	0,00	-0,13	0,46	-0,12	0,37
PFKM	0,001	0,10	3E-19	0	1E-05		-0,08	-0,22	0,10	0,35	0,26	0,28	0,22	0,37	0,34	0,23	0,32	-0,13	0,21	-0,04
PFKL	0,21	0,24	0,09	0,0008	0,0005	0,02		0,07	0,14	0,10	-0,06	0,05	0,04	0,12	0,02	-0,10	-0,14	0,00	-0,19	0,06
PFKFB3	2E-06	5E-06	0,71	1E-09	7E-08	1E-09	0,07		-0,07	-0,14	-0,10	-0,16	-0,26	-0,18	-0,01	-0,07	-0,08	0,25	-0,10	-0,01
ALDOA	1E-05	3E-06	0,57	1E-15	1E-08	0,0042	8E-05	0,04		0,34	0,37	0,40	0,38	0,30	0,14	0,23	-0,14	0,17	-0,21	0,22
TPI1	3E-06	0,17	3E-12	9E-42	0,84	3E-23	0,004	0,0001	4E-22		0,54	0,51	0,49	0,52	0,39	0,29	0,10	0,08	-0,11	-0,06
GAPDH	2E-12	3E-12	4E-11	4E-39	0,31	7E-13	0,09	0,004	2E-26	0		0,36	0,31	0,27	0,39	0,33	0,14	0,17	0,07	-0,04
PGK1	4E-18	1E-06	4E-05	7E-18	0,00	5E-15	0,14	5E-06	4E-30	0	2E-24		0,59	0,49	0,24	0,44	-0,02	0,15	-0,10	0,13
PGAM1	5E-10	3E-08	0,01	4E-23	0,70	3E-10	0,24	4E-13	5E-28	0	9E-19	0		0,46	0,31	0,33	-0,08	0,03	-0,09	0,01
ENO1	0,06	0,09	1E-21	3E-28	0,16	9E-27	0,001	8E-07	3E-17	0	2E-14	0	5E-41		0,30	0,50	0,26	0,002	-0,19	-0,02
PKM2	0,31	6E-08	1E-18	2E-37	0,14	3E-22	0,60	0,88	0,0001	2E-29	2E-29	1E-11	5E-18	2E-17		0,11	0,03	0,16	0,25	-0,08
LDHA	1E-24	1E-06	2E-17	2E-27	0,98	2E-10	0,004	0,07	1E-10	6E-16	7E-21	2E-38	1E-20	0	0,002		0,29	0,09	-0,11	0,004
c-Myc	0,42	0,02	2E-26	6E-13	0,0005	1E-19	8E-05	0,04	9E-05	0,008	6E-05	0,51	0,03	2E-13	0,45	2E-16		-0,17	0,01	-0,23
HIF1α	0,0002	1E-06	1E-09	0,47	4E-41	0,0004	0,91	6E-12	2E-06	0,04	2E-06	5E-05	0,40	0,97	6E-06	0,01	3E-06		0,004	0,24
AMPKα1	0,001	0,09	0,03	5E-10	0,001	3E-09	8E-08	0,004	3E-09	0,002	0,06	0,008	0,009	1E-07	2E-12	0,003	0,88	0,91		-0,07
AMPKα2	0,0002	0,67	0,16	7E-06	2E-26	0,2732	0,08	0,81	5E-10	0,12	0,30	0,0004	0,85	0,56	0,03	0,91	1E-10	3E-11	0,07	

FIGURE 4 PRL-3-driven glycolysis is not mediated by AMPK, HIF-1α, and c-Myc. A, PRL-3-INA-6, C104S-INA-6, and mock cells grown in hypoxia or normoxia for 4 or 24 h and immunoblotted with antibodies against HIF-1α and PRL-3. B, Glycolysis was analyzed in PRL-3-INA-6 and mock cells grown in hypoxia and normoxia for 4 days. C, PRL-3-INA-6, C104S-INA-6, and mock cells were cultured with serum- and IL-6-containing medium or in 0.1 % BSA without IL-6 for 4 h and immunoblotted with antibodies against PRL-3, phosph-thr-172 AMPK, total AMPK, and c-Myc. D, AMPK was knocked down in PRL-3-INA-6 and mock cells by transient transfection using two different siRNAs against AMPKα1 and AMPKα2. Glycolysis parameters were measured by Seahorse. E, Protein lysates were prepared from the same cells and AMPKα and PRL-3 protein level was measured by Western blot. F, PTP4A3 (PRL-3) gene expression is positively correlated with expression of several genes involved in glycolysis in MM cells. Spearman correlation coefficients (green) and their respective *p*-values (blue) between the levels of mRNA for PRL-3 and glycolysis enzymes, and a few other relevant molecules in 767 samples of purified MM cells from patient bone marrow. Data are derived from the CoMMpass study (IA12). Darker green and darker blue indicate higher Spearman correlation coefficient and lower *p*-value, respectively

However, also in hypoxia, there was a large difference in glycolysis between PRL-3-INA-6 and mock cells (Figure 4B, Figure S6). These observations argue against PRL-3 as a mediator of HIF-1α-driven glycolysis. Both activation and total level of AMPK were reduced in PRL-3-INA-6 (Figure 4C). Knockdown of AMPK reduced glycolysis in both PRL-3-INA-6 and Mock-INA-6 (Figure 4D,E). The observed PRL-3-induced reduction of AMPK can, therefore, best be explained as a negative feedback reaction to the PRL-3-driven increase in glycolysis.

Figure 4F shows correlations between expression of the PRL-3 gene *PTP4A3*, a selection of key genes regulating glycolysis (*c-myc*, *HIF1α*, *AMPKα1*, and *AMPKα2*) and genes encoding glycolytic enzymes in the CoMMpass MM dataset (Interim analysis (IA) 12, n = 767). Interestingly, there was a trend for the glycolytic enzymes to have a positive correlation with either *PTP4A3* or *c-myc* expression. *PTP4A3* correlated most significantly with *GAPDH*, *PGK1*, *PGAM1*, and *LDHA*, whereas *c-myc* correlated with *HK2*, *GPI*, *PFKM*, *ENO1*, and *LDHA*. This supports that upregulation of enzymes involved in glycolysis partly explains higher glycolysis rate in PRL-3-overexpressing cells.

3.7 | PRL-3 regulates the serine/glycine pathway

All the enzymes involved in serine synthesis [phosphoglycerate dehydrogenase (PHGDH), phosphoserine aminotransferase (PSAT1), and phosphoserine phosphatase (PSPH)] were expressed in INA-6 and JJN-3, and together with methylenetetrahydrofolate dehydrogenase 2 (MTHFD2) were more expressed in cells with overexpression of PRL-3 (Figure 5A, Figure S7, and Figure 3A). MTHFD2 is a mitochondrial enzyme that contributes to the synthesis of glycine by regenerating the cofactor tetrahydrofolate (THF) needed for the serine hydroxymethyl transferase (SHMT)-2 driven conversion of serine to glycine.

Another molecule highly upregulated in PRL-3-INA-6, particularly after a 12-hour culture without IL-6 (Figures 3A and 5A), was the transporter of neutral amino acids, CD98, encoded by *SLC3A2* and *SLC7A5*.

In an effort to directly demonstrate the influence of PRL-3 on the serine/glycine pathway, we measured the level of carbon derived from glucose in serine and glycine in PRL-3 and Mock-INA-6 cells by NMR spectroscopy

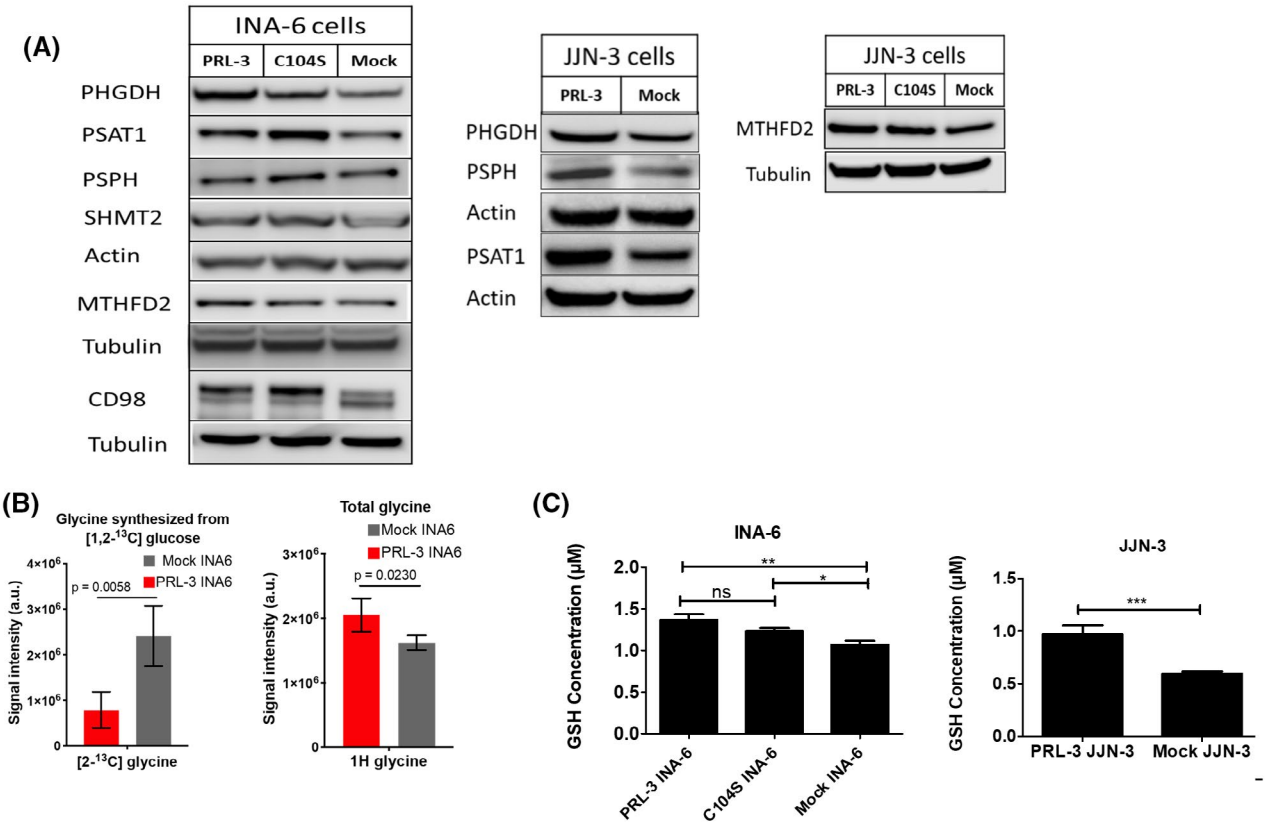

FIGURE 5 PRL-3 regulates serine/glycine synthesis pathway. A, INA-6 and JJN-3 cells overexpressing wild type (WT) or catalytically dead mutant (C104S) PRL-3, and mock control cells were immunoblotted with indicated antibodies. INA-6 cells were starved of IL-6 before cell harvest to reduce endogenous levels of PRL-3. B, Glycine synthesized from [1,2-^{13}C] glucose (left) and total glycine (right) as measured by NMR. n = 4. C, Level of GSH was measured in PRL-3-INA-6, C104S-INA-6, PRL-3-JJN-3 cells, and their respective mock cells. Results are mean of two independent experiments each with minimum two replicates. Error bars show SD. ns, not significant, $*P \leq .05$, $**P \leq .01$, $***P \leq .001$

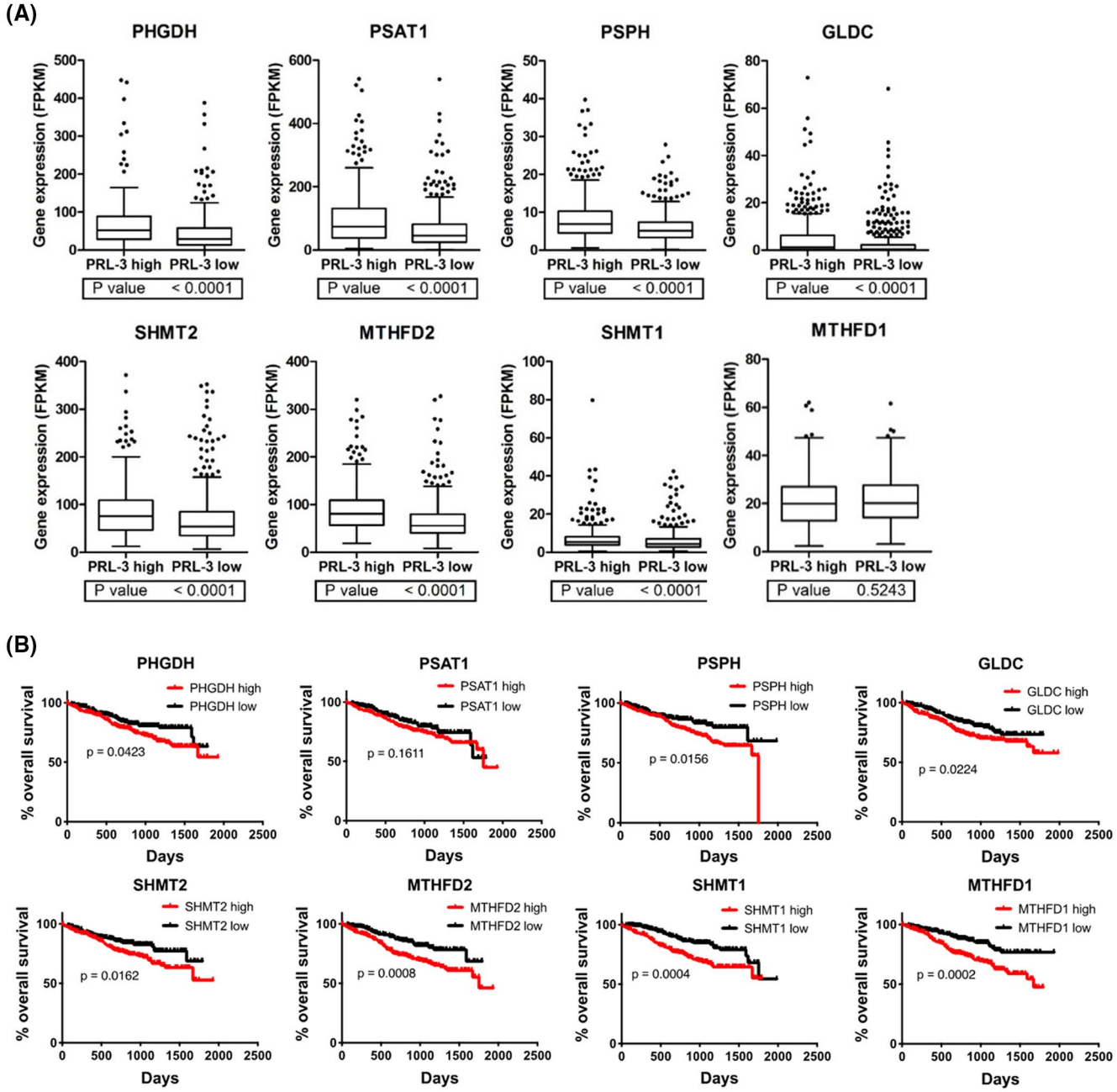

FIGURE 6 Correlation between expression of PRL-3 and serine/glycine pathway enzymes in primary myeloma cells. A, Seven hundred and sixty-seven samples of purified MM cells from patient bone marrow from the CoMMpass study (IA12) were divided in two equal groups, expressing high or low levels of PRL-3 mRNA. Expression levels of serine/glycine pathway genes in the two groups were compared. B, Kaplan-Meier plots showing overall survival of patients with high or low expression of enzymes involved in serine/glycine pathway. Data from the CoMMpass data bank, IA12

after culturing cells without serine and glycine and with 1,2-$^{13}C_2$-glucose as the only form of glucose. Unfortunately, intracellular serine was below the detection limit in both PRL-3- and Mock-INA-6. The level of glycine with carbon derived from glucose was much higher in Mock-INA-6 than in PRL-3-INA-6, whereas total glycine content was higher in PRL-3-INA-6 (Figure 5B). These results suggest that serine-derived glycine is rapidly degraded by GLDC in PRL-3-expressing cells for one-carbon delivery. Intracellular [1,2-^{13}C] glucose and [2,3-^{13}C] lactate levels were also higher in PRL-3-INA-6, again confirming the increased glycolytic flux (Figure S8).

Consistent with an increased activity in the serine/glycine pathway, there were significantly higher levels of GSH, a molecule dependent on glycine for production, in both INA-6 and JJN-3 cells overexpressing PRL-3 than in mock cells (Figure 5C). However, we cannot exclude the possibility that increase in GSH also could reflect a change in the cells' redox potential.

TABLE 1 Gene set enrichment analysis shows enrichment of genes involved in amino acid metabolism in cells with high PRL-3 mRNA levels

A					
Rank	**Pathway commons: Reactome gene set**	**ES**	**NES**	***P*-value (FDR corrected)**	**Number of genes used**
1	PTM: gamma carboxylation, hypusine formation, and arylsulfatase activation	0.66	2.26	<.0001	30
2	**Amino acid and derivative metabolism**	**0.55**	**2.24**	**.022**	**188**
3	Antigen processing-Cross presentation	0.66	2.23	.022	81
4	Regulation of Complement cascade	0.69	2.19	<.0001	23
5	ER-Phagosome pathway	0.71	2.13	.032	64
6	Antigen Presentation: Folding, assembly, and peptide loading of class I MHC	0.76	2.12	.022	23
7	**Amino acid synthesis and interconversion (transamination)**	**0.89**	**2.08**	**<.0001**	**13**
8	Metabolism of steroid hormones and vitamin D	0.61	2.08	<.0001	28
9	Steroid hormones	0.61	2.08	<.0001	28
10	Gamma-carboxylation, transport, and amino-terminal cleavage of proteins	0.76	2.06	<.0001	13
49	**Serine biosynthesis**	**0.99**	**1.55**	**.043**	**3**
B					
Gene	**Fold change**				
PHGDH	**1.51**				
PSAT1	**1.51**				
PSPH	**1.42**				
ASNS	1.36				
GPT2	1.29				
GOT2	1.22				
PYCR1	1.21				
GOT1	1.18				
OAT	1.17				
CCBL1	1.14				
ALDH18A1	1.11				
GLUD1	1.05				
GPT	0.99				

Note: Seven hundred and sixty-seven samples from the CoMMpass study of purified MM cells were divided in two groups with high or low levels of PRL-3 mRNA. A, A total of 1442 gene sets derived from the Reactome pathway database were analyzed for enrichment in samples with high PRL-3 levels and ranked according to normalized enrichment score (NES). Terms related to amino acid synthesis and metabolism are shown in bold. B, Genes in gene set called "Amino acid synthesis and interconversion (transamination)" ranked according to fold change in expression between PTP4A3 high and low samples. All the enzymes involved in serine synthesis pathway are shown in bold.

Abbreviations: ER, enrichment score; FDR, false discovery rate.

3.8 | Correlation between expression of PRL-3 and serine/glycine pathway enzymes in primary myeloma cells

To examine whether PRL-3 expression correlated with expression of enzymes in the serine/glycine pathway, we dichotomized 767 samples of purified myeloma cells from IA12 of the CoMMpass study according to *PTP4A3* expression. *PHGDH*, *PSAT1*, and *PSPH*, had on average higher expression in samples with high levels of *PTP4A3*. Genes encoding mitochondrial enzymes, *SHMT2*, *MTHFD2*, and *GLDC*, showed the same pattern, whereas *SHMT1* and *MTHFD1*, cytosolic isoforms of these enzymes, showed lower, albeit significant (*SHMT1*) or no covariation (*MTHFD1*) with *PTP4A3* (Figure 6A).

Interestingly, similarly as previously shown for PRL-3 mRNA,[23] high levels of mRNAs for the majority of these enzymes predicted reduced overall survival time (Figure 6B). In contrast, *c-myc* mRNA had no prognostic value (Figure S9).

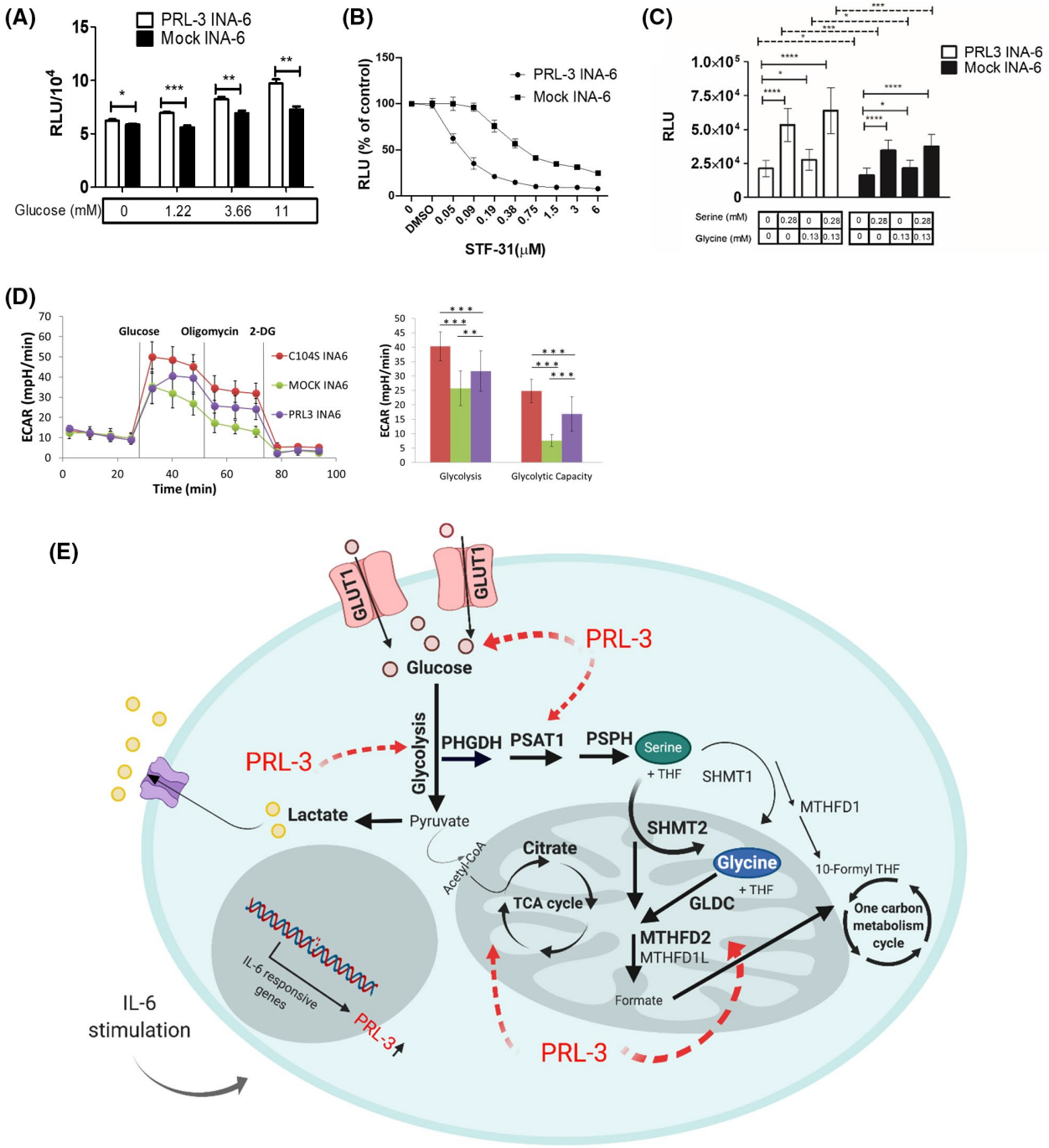

FIGURE 7 PRL-3 enables cells to utilize exogenous nutrients and its effect on metabolism is not dependent on PRL-3's phosphatase activity. A, ATP levels were measured using the Cell Titer-Glo (CTG) assay after lysing the same number of PRL-3-INA-6 and mock cells grown in various concentrations of glucose for 24 h. The plot shows one representative out of three independent experiments with triplicates. B, Proliferation was measured after seeding PRL-3-INA-6 and mock cells overnight with increasing doses of the GLUT1 inhibitor STF-31. The plot is one representative out of three independent experiments with three replicates each. C, Proliferation was measured after seeding PRL-3-INA-6 and mock cells overnight with indicated serine and glycine concentrations. The plot shows mean of three independent experiments with four replicates each. D, Glycolysis was measured by Seahorse XF Analyzer in INA-6 cells overexpressing wild type (PRL-3-INA-6) and catalytically dead PRL-3 (C104S-PRL-3) and mock control cells. Seahorse graph is one representative out of two independent experiments, each with 24 technical replicates. Error bars show ± SD. *$P \leq .05$, **$P \leq .01$, ***$P \leq .001$, ***$P \leq .001$, ****$P \leq .0001$. E, Schematic illustration of current results. PRL-3, mediator of IL-6, promotes the serine/glycine pathway and induces aerobic glycolysis, the latter partly through upregulation of glycolytic enzymes and GLDC. Figure is created with BioRender

Reactome pathway analysis was done for differentially expressed genes in patients with high versus low *PTP4A3* expression in the CoMMpass cohort. Genes relevant for amino acid metabolism had a particularly high normalized enrichment score in high *PTP4A3* samples. (Table 1A). When the genes in "Amino acid synthesis and interconversion (transamination)" with 13 genes, were ranked according to fold change, the three enzymes involved in serine biosynthesis, PHGDH, PSAT1, and PSPH, were the top three genes (Table 1B).

3.9 | PRL-3 enables cells to utilize exogenous nutrients but makes INA-6 cells vulnerable to GLUT1 inhibition

The PRL-3-mediated increase in glucose- and amino acid transporters, suggested that cells with PRL-3 would be better prepared to exploit exogenous nutrients. We grew INA-6 cells without or in the presence of increasing concentration of glucose and measured ATP production. In the absence of glucose, there was almost no difference in ATP production between PRL-3-INA-6 and Mock-INA-6 (Figure 7A). Whereas PRL-3-INA-6 showed a glucose-dependent increase in ATP production, mock cells apparently were unable to use increased levels of exogenous glucose to enhance their ATP production. Interestingly, STF-31, an inhibitor of GLUT1, blocked the proliferation of PRL-3-INA-6 much more efficiently than proliferation of the mock cells (Figure 7B).

To see whether PRL-3 enabled cells to utilize exogenous serine and glycine, we cultured PRL-3-INA-6 and Mock-INA-6 in medium with and without glycine and serine and measured cell proliferation. Exogenous serine was permissive for increased proliferation of both PRL-3 and mock cells, but less so for mock cells. In contrast to serine, glycine did not increase proliferation much, neither in the absence, nor in the presence of serine (Figure 7C).

3.10 | Non-phosphatase mutant PRL-3 is actively regulating glycolysis

In many of the experiments, myeloma cells overexpressing a phosphatase-dead mutant of PRL-3 behaved like cells with WT PRL-3 (Figures 3B,C and 5A). Consistent data were seen in Seahorse experiments (Figure 7D). These experiments indicate that the metabolic switch induced by PRL-3 is not dependent on PRL-3's phosphatase activity.

4 | DISCUSSION

Cancer cells can adapt their metabolism to the demands of a growing tumor. Increased glycolytic flux and changes in amino acid metabolism are central to these alterations.[44] This study adds PRL-3 to the list of important metabolic regulators in cancer. PRL-3 stimulated glycolysis and other metabolic processes without increasing proliferation, demonstrating that microenvironment signaling molecules, such as IL-6, can alter metabolism via signals that can be separated from proliferative signaling. Figure 7E shows an overview of the PRL-3 effects described in this paper.

A metabolic switch from OXPHOS to aerobic glycolysis, called the Warburg effect, is a cancer hallmark.[45] This leads to increased production of pyruvate, which in healthy cells is oxidized in the TCA cycle to provide reducing power for OXPHOS. In cancer cells, pyruvate is typically reduced to lactate, supplying carbon units for the synthesis of biomolecules required for cell growth.[46]

In our experiments, PRL-3 potently induced aerobic glycolysis, OXPHOS, and thereby, ATP production in hematopoietic cancer cells. Upregulation of GLUT1 and CD98, transporters for glucose and neutral amino acids, respectively, allowed increased use of exogenous nutrients. PRL-3 increased import of glucose, but at the cost of making cells more dependent on glucose for survival, reflected in the vulnerability of PRL-3-expressing INA-6 cells to the GLUT1 inhibitor STF-31, a finding that may be of clinical significance.

Enzymes catalyzing glycolysis and the serine/glycine pathway, a side path of glycolysis, were upregulated by PRL-3. Glycine consumption and expression of enzymes in the mitochondrial serine/glycine biosynthetic pathway are another important adaptation in cancer metabolism and strongly correlated with proliferation rates between different cancer cells.[47] In contrast to healthy cells, where serine/glycine production mostly occurs in cytosol, cancer cells predominately produce these amino acids in mitochondria, regulated by enzymes only found at low levels in adult tissues.[48] In our cells, PRL-3 mainly upregulated mitochondrial isoforms of enzymes with both a cytosolic and a mitochondrial paralog. We found a positive correlation between expression of *PTP4A3* and genes encoding mitochondrial serine/glycine enzymes. Enriched expression of serine synthesis pathway genes in MM cells from patients with high expression of the PRL-3 gene, indicates clinical relevance of our cell line findings.

GLDC was the enzyme most upregulated by PRL-3. The importance of high levels of GLDC for cancer cells was demonstrated in a glioblastoma model.[49] If GLDC activity was inhibited by shRNA, there was a sharp reduction in cell viability, most likely due to conversion of accumulating glycine to toxic metabolites.

Although we cannot completely rule out reduced production of glycine, we think high glycine turnover by GLDC activity was likely the cause of the low glucose-derived glycine content in PRL-3-INA-6 cells after depletion of exogenous serine and glycine. Exogenous glycine cannot be used for production of one-carbon units but can be converted to serine.[50]

The higher total level of glycine in PRL3-overexpressing cells than in mock cells can, therefore, be interpreted as remnants of exogenous glycine. The necessity of converting glycine to serine is probably lower in PRL-3-expressing cells than in mock cells, since the capacity to produce serine from glucose is higher than in mock cells.

GLDC is a regulator of glycolysis.[39-41] It promotes glycolysis in non-small cell lung carcinoma[41] and in pluripotent stem cells.[39] GLDC knockdown in our MM cells gave reduced glycolysis, identifying GLDC as one of the mediators of PRL-3-driven glycolysis.

Consistent with our findings, in a report by Xu et al., PRL-3 promoted glycose uptake and lactate export.[51] In colorectal cancer cells, they found upregulation of GLUT1 and the glycolytic enzymes HK2, PKM2, and LDHA, largely in line with our results in MM cells.

Higher ATP production in vitro and increased tumor growth in vivo in B16 murine melanoma cells that forcibly expressed PRL-3 have been previously reported.[52] They argue that PRLs bind directly to a membrane protein involved in magnesium homeostasis, CNNMs, which increases intracellular Mg^{2+} levels[53] and influences metabolism.[14,52] However, the phosphatase-dead PRL-3 mutant C104S was not able to bind CNNM and had no effect on ATP production. This contrasts with our experiments where C104S was almost as effective as WT PRL-3 in regulating metabolism. Since C104S-PRL-3 cannot bind CNNM proteins,[16,52] the potent influence of C104S on metabolism could be an indication that PRL-3 does not promote glycolysis and the serine synthesis pathway primarily by binding to CNNMs. We were not able to pinpoint a specific mechanism for the metabolic adaptation in our work. We find it probable that the metabolic adaptation observed in the myeloma cells is due to changes in the expression or stability of key metabolic proteins. This could happen through changes in gene expression, for example as the consequence of the direct interaction between PRL-3 and histone demethylases as shown by Liu et al.[54] and Zhang et al.[55] or through the activation of transcription factors such as STAT3, as shown by us and others.[23,25]

The Warburg effect is promoted when the transcription factor HIF-1α is inappropriately stabilized in cells during normoxia.[43] There was no PRL-3-mediated stabilization of HIF-1α in INA-6 cells overexpressing PRL-3, arguing against HIF-1α as a downstream mediator of the PRL-3-driven glycolysis. HIF-1α was strongly induced in INA-6 cells during hypoxia but was not influenced by PRL-3, and PRL-3 was not induced by hypoxia. Overall, this shows that hypoxia (HIF-1α) and PRL-3 promote glycolysis by distinct mechanisms.

AMPK is another important regulator of cellular metabolism.[56] PRL-3 reduced activation of AMPK in our cells. AMPK is normally activated by cellular stress like depletion of nutrients or a low ratio of ATP over AMP/ADP, and it promotes catabolic processes.[56] AMPK reportedly enhances glycolysis in endothelial cells and in rat muscle cells,[57,58] consistent with the reduced glycolytic rate after knockdown of AMPK in our study. PRL-3-induced AMPK deactivation was most probably the result of a more favorable energy situation caused by PRL-3 in our cells.

The transcription factor c-Myc, another important regulator of metabolism,[43] is often overexpressed in myeloma.[59] We saw no induction of c-Myc by PRL-3 and the CoMMpass data did not suggest co-regulation of *PTP4A3* and *c-myc*. There was correlation between expression of *c-myc* and a few genes involved in glycolysis, but in general not the genes that correlated with *PTP4A3* expression. A similar complementary pattern of correlations was seen for the serine/glycine pathway, where *c-myc* correlated with the genes for two cytosolic enzymes, the only two genes that did not correlate with *PTP4A3* expression (Data not shown).

Even though many phosphatase-dependent functions are reported for PRLs,[60,61] still an interesting and disputed topic in the study of the PRL family of proteins is whether they are in fact phosphatases or pseudo-phosphatases in vivo with some residual phosphatase activity in vitro. It has been difficult to convincingly identify direct substrates for PRLs in vivo[18] and biological effects of PRLs that are not dependent on phosphatase activity, have been demonstrated.[26,62] In the interaction between the PRLs and the magnesium-regulatory proteins of the CNNM family, PRLs acts as pseudophosphatases.[16,63] In the present study, the phosphatase-dead C104S mutant PRL-3 was as potent as WT PRL-3 in most of the experiments. As an example, phosphatase-dead PRL-3-stimulated aerobic glycolysis to the same extent as WT PRL-3. In a previous study, we saw that C104S mutant PRL-3 was a weaker (but significant) inhibitor of MM cell apoptosis than WT PRL-3, but could not cause phosphorylation of Src.[26] Clearly, a phosphatase-dead PRL-3 mutant has important biological effects like those of WT PRL-3. The large influence of PRL-3 on protein expression could lead to the suspicion that it acts as a transcription factor, and this was reported in a recent paper.[64]

In summary, this study establishes a role for PRL-3 as an important regulator of metabolism in cancer cells of hematological origin. Most notably, PRL-3 promotes the serine/glycine pathway and induces aerobic glycolysis, the latter partly through upregulation of glycolytic enzymes and GLDC, but independently of HIF-1α, c-Myc, and AMPK. PRL-3 emerges as an attractive target in treatment directed against cancer metabolism.

ACKNOWLEDGMENTS

The authors thank Hanne Hella, Berit Størdal, Glenn Buene, and Ida Eide Langørgen for excellent technical support. Part of the work has been performed at the MR Core Facility and the Proteomics and Modomics Experimental Core Facility,

Norwegian University of Science and Technology (NTNU). The core facilities are funded by the Faculty of Medicine and Health Sciences at NTNU and Central Norway Regional Health Authority. The authors acknowledge Multiple Myeloma Research Foundation Personalized Medicine Initiatives (https://research.themmrf.org and www.themmrf.org). This project was funded by the NTNU and the Liaison Committee for Education, Research, and Innovation in Central Norway.

CONFLICT OF INTEREST

There is no conflict of interest to disclose.

AUTHOR CONTRIBUTIONS

P. Abdollahi and E.N. Vandsemb were instrumental in study design, lab work, and in writing the manuscript. S. Elsaadi and L.M. Røst contributed to study design, lab work, and in writing the manuscript. M.A. Hjort, S. Moestue, T. Andreassen, and K. Misund did lab work and reviewed the manuscript. R. Yang, T.S. Slørdahl, T.B. Rø, A.M. Sponaas, and P. Bruheim contributed to study planning and reviewed the manuscript. M. Børset conceptualized and coordinated the study and wrote the manuscript.

REFERENCES

1. Saha S, Bardelli A, Buckhaults P, et al. A phosphatase associated with metastasis of colorectal cancer. *Science*. 2001;294:1343-1346.
2. Bardelli A, Saha S, Sager JA, et al. PRL-3 expression in metastatic cancers. *Clin Cancer Res*. 2003;9:5607-5615.
3. Miskad UA, Semba S, Kato H, Yokozaki H. Expression of PRL-3 phosphatase in human gastric carcinomas: close correlation with invasion and metastasis. *Pathobiology*. 2004;71:176-184.
4. Polato F, Codegoni A, Fruscio R, et al. PRL-3 phosphatase is implicated in ovarian cancer growth. *Clin Cancer Res*. 2005;11:6835-6839.
5. Radke I, Gotte M, Kersting C, Mattsson B, Kiesel L, Wulfing P. Expression and prognostic impact of the protein tyrosine phosphatases PRL-1, PRL-2, and PRL-3 in breast cancer. *Br J Cancer*. 2006;95:347-354.
6. Vandsemb EN, Bertilsson H, Abdollahi P, et al. Phosphatase of regenerating liver 3 (PRL-3) is overexpressed in human prostate cancer tissue and promotes growth and migration. *J Transl Med*. 2016;14:71.
7. Fagerli UM, Holt RU, Holien T, et al. Overexpression and involvement in migration by the metastasis-associated phosphatase PRL-3 in human myeloma cells. *Blood*. 2008;111:806-815.
8. Hjort MA, Hov H, Abdollahi P, et al. Phosphatase of regenerating liver-3 (PRL-3) is overexpressed in classical Hodgkin lymphoma and promotes survival and migration. *Exp Hematol Oncol*. 2018;7:8.
9. Hjort MA, Abdollahi P, Vandsemb EN, et al. Phosphatase of regenerating liver-3 is expressed in acute lymphoblastic leukemia and mediates leukemic cell adhesion, migration and drug resistance. *Oncotarget*. 2018;9:3549-3561.
10. Park JE, Yuen HF, Zhou JB, et al. Oncogenic roles of PRL-3 in FLT3-ITD induced acute myeloid leukaemia. *EMBO Mol Med*. 2013;5:1351-1366.
11. Qu S, Liu B, Guo X, et al. Independent oncogenic and therapeutic significance of phosphatase PRL-3 in FLT3-ITD-negative acute myeloid leukemia. *Cancer*. 2014;120:2130-2141.
12. Zhou J, Bi C, Chng WJ, et al. PRL-3, a metastasis associated tyrosine phosphatase, is involved in FLT3-ITD signaling and implicated in anti-AML therapy. *PLoS One*. 2011;6:e19798.
13. Zhou J, Cheong LL, Liu SC, et al. The pro-metastasis tyrosine phosphatase, PRL-3 (PTP4A3), is a novel mediator of oncogenic function of BCR-ABL in human chronic myeloid leukemia. *Mol Cancer*. 2012;11:72.
14. Hardy S, Kostantin E, Wang SJ, et al. Magnesium-sensitive upstream ORF controls PRL phosphatase expression to mediate energy metabolism. *Proc Natl Acad Sci U S A*. 2019;116(8):2925-2934.
15. Funato Y, Miki H. Molecular function and biological importance of CNNM family Mg2+ transporters. *J Biochem*. 2019;165(3):219-225.
16. Zhang H, Kozlov G, Li X, Wu H, Gulerez I, Gehring K. PRL3 phosphatase active site is required for binding the putative magnesium transporter CNNM3. *Sci Rep*. 2017;7:48.
17. Gulerez I, Funato Y, Wu H, et al. Phosphocysteine in the PRL-CNNM pathway mediates magnesium homeostasis. *EMBO Rep*. 2016;17:1890-1900.
18. Hardy S, Kostantin E, Hatzihristidis T, Zolotarov Y, Uetani N, Tremblay ML. Physiological and oncogenic roles of the PRL phosphatases. *FEBS J*. 2018;285:3886-3908.
19. Klein B, Zhang XG, Jourdan M, et al. Paracrine rather than autocrine regulation of myeloma-cell growth and differentiation by interleukin-6. *Blood*. 1989;73:517-526.
20. Klein B, Zhang XG, Lu ZY, Bataille R. Interleukin-6 in human multiple myeloma. *Blood*. 1995;85:863-872.
21. Rathmell JC, Vander Heiden MG, Harris MH, Frauwirth KA, Thompson CB. In the absence of extrinsic signals, nutrient utilization by lymphocytes is insufficient to maintain either cell size or viability. *Mol Cell*. 2000;6:683-692.
22. Bauer DE, Harris MH, Plas DR, et al. Cytokine stimulation of aerobic glycolysis in hematopoietic cells exceeds proliferative demand. *FASEB J*. 2004;18:1303-1305.
23. Chong PSY, Zhou J, Lim JSL, et al. IL6 promotes a STAT3-PRL3 feedforward loop via SHP2 repression in multiple myeloma. *Can Res*. 2019;79:4679-4688.
24. Wu SP, Pfeiffer RM, Ahn IE, et al. Impact of genes highly correlated with MMSET myeloma on the survival of non-MMSET myeloma patients. *Clin Cancer Res*. 2016;22:4039-4044.
25. Slørdahl TS, Abdollahi P, Vandsemb EN, et al. The phosphatase of regenerating liver-3 (PRL-3) is important for IL-6-mediated survival of myeloma cells. *Oncotarget*. 2016;7:27295-27306.
26. Abdollahi P, Vandsemb EN, Hjort MA, et al. Src family kinases are regulated in multiple myeloma cells by phosphatase of regenerating liver-3. *Mol Cancer Res*. 2017;15:69-77.
27. Campeau E, Ruhl VE, Rodier F, et al. A versatile viral system for expression and depletion of proteins in mammalian cells. *PLoS One*. 2009;4:e6529.
28. Søgaard CK, Blindheim A, Røst LM, et al. "Two hits - one stone"; increased efficacy of cisplatin-based therapies by targeting PCNA's role in both DNA repair and cellular signaling. *Oncotarget*. 2018;9:32448-32465.
29. Wessel D, Flugge UI. A method for the quantitative recovery of protein in dilute solution in the presence of detergents and lipids. *Anal Biochem*. 1984;138:141-143.

30. Geiger T, Wisniewski JR, Cox J, et al. Use of stable isotope labeling by amino acids in cell culture as a spike-in standard in quantitative proteomics. *Nat Protoc*. 2011;6:147-157.
31. Boutet E, Lieberherr D, Tognolli M, et al. UniProtKB/Swiss-Prot, the manually annotated section of the uniprot knowledgebase: how to use the entry view. *Methods Mol Biol*. 2016;1374:23-54.
32. Kall L, Canterbury JD, Weston J, Noble WS, MacCoss MJ. Semi-supervised learning for peptide identification from shotgun proteomics datasets. *Nat Methods*. 2007;4:923-925.
33. Ong SE, Blagoev B, Kratchmarova I, et al. Stable isotope labeling by amino acids in cell culture, SILAC, as a simple and accurate approach to expression proteomics. *Mol Cell Proteomics*. 2002;1:376-386.
34. Hochberg Y, Benjamini Y. More powerful procedures for multiple significance testing. *Stat Med*. 1990;9:811-818.
35. Tyanova S, Temu T, Sinitcyn P, et al. The Perseus computational platform for comprehensive analysis of (prote)omics data. *Nat Methods*. 2016;13:731-740.
36. Austdal M, Skrastad RB, Gundersen AS, Austgulen R, Iversen AC, Bathen TF. Metabolomic biomarkers in serum and urine in women with preeclampsia. *PLoS One*. 2014;9:e91923.
37. Bettum IJ, Gorad SS, Barkovskaya A, et al. Metabolic reprogramming supports the invasive phenotype in malignant melanoma. *Cancer Lett*. 2015;366:71-83.
38. Barretina J, Caponigro G, Stransky N, et al. The Cancer Cell Line Encyclopedia enables predictive modelling of anticancer drug sensitivity. *Nature*. 2012;483:603-607.
39. Kang PJ, Zheng J, Lee G, et al. Glycine decarboxylase regulates the maintenance and induction of pluripotency via metabolic control. *Metab Eng*. 2019;53:35-47.
40. Woo CC, Kaur K, Chan WX, Teo XQ, Lee THP. Inhibiting glycine decarboxylase suppresses pyruvate-to-lactate metabolism in lung cancer cells. *Front Oncol*. 2018;8:196.
41. Zhang WC, Shyh-Chang N, Yang H, et al. Glycine decarboxylase activity drives non-small cell lung cancer tumor-initiating cells and tumorigenesis. *Cell*. 2012;148:259-272.
42. Locasale JW. Serine, glycine and one-carbon units: cancer metabolism in full circle. *Nat Rev Cancer*. 2013;13:572-583.
43. Cantor JR, Sabatini DM. Cancer cell metabolism: one hallmark, many faces. *Cancer Discov*. 2012;2:881-898.
44. Yang M, Vousden KH. Serine and one-carbon metabolism in cancer. *Nat Rev Cancer*. 2016;16:650-662.
45. Warburg O. On respiratory impairment in cancer cells. *Science*. 1956;124:269-270.
46. Ganapathy-Kanniappan S. Molecular intricacies of aerobic glycolysis in cancer: current insights into the classic metabolic phenotype. *Crit Rev Biochem Mol Biol*. 2018;53:667-682.
47. Jain M, Nilsson R, Sharma S, et al. Metabolite profiling identifies a key role for glycine in rapid cancer cell proliferation. *Science*. 2012;336:1040-1044.
48. Nilsson R, Jain M, Madhusudhan N, et al. Metabolic enzyme expression highlights a key role for MTHFD2 and the mitochondrial folate pathway in cancer. *Nat Commun*. 2014;5:3128.
49. Kim D, Fiske BP, Birsoy K, et al. SHMT2 drives glioma cell survival in ischaemia but imposes a dependence on glycine clearance. *Nature*. 2015;520:363-367.
50. Labuschagne CF, van den Broek NJ, Mackay GM, Vousden KH, Maddocks OD. Serine, but not glycine, supports one-carbon metabolism and proliferation of cancer cells. *Cell Rep*. 2014;7:1248-1258.
51. Xu H, Zeng Y, Liu L, et al. PRL-3 improves colorectal cancer cell proliferation and invasion through IL-8 mediated glycolysis metabolism. *Int J Oncol*. 2017;51:1271-1279.
52. Funato Y, Yamazaki D, Mizukami S, Du L, Kikuchi K, Miki H. Membrane protein CNNM4-dependent Mg2+ efflux suppresses tumor progression. *J Clin Invest*. 2014;124:5398-5410.
53. Funato Y, Yoshida A, Hirata Y, Hashizume O, Yamazaki D, Miki H. The Oncogenic PRL protein causes acid addiction of cells by stimulating lysosomal exocytosis. *Dev Cell*. 2020;55(4):387-397.e8.
54. Liu Y, Zheng P, Liu Y, et al. An epigenetic role for PRL-3 as a regulator of H3K9 methylation in colorectal cancer. *Gut*. 2013;62:571-581.
55. Zhang M, Wei Y, Liu Y, et al. Metastatic phosphatase PRL-3 induces ovarian cancer stem cell sub-population through phosphatase-independent deacetylation modulations. *iScience*. 2020;23(1):100766.
56. Carling D. AMPK signalling in health and disease. *Curr Opin Cell Biol*. 2017;45:31-37.
57. Holmes BF, Kurth-Kraczek EJ, Winder WW. Chronic activation of 5'-AMP-activated protein kinase increases GLUT-4, hexokinase, and glycogen in muscle. *J Appl Physiol*. 1999;87:1990-1995.
58. Yang Q, Xu J, Ma Q, et al. PRKAA1/AMPKalpha1-driven glycolysis in endothelial cells exposed to disturbed flow protects against atherosclerosis. *Nat Commun*. 2018;9:4667.
59. Avet-Loiseau H, Gerson F, Magrangeas F, Minvielle S, Harousseau JL, Bataille R. Rearrangements of the c-myc oncogene are present in 15% of primary human multiple myeloma tumors. *Blood*. 2001;98:3082-3086.
60. Lujan P, Varsano G, Rubio T, et al. PRL-3 disrupts epithelial architecture by altering the post-mitotic midbody position. *J Cell Sci*. 2016;129:4130-4142.
61. Li Q, Bai Y, Lyle LT, et al. Mechanism of PRL2 phosphatase-mediated PTEN degradation and tumorigenesis. *Proc Natl Acad Sci U S A*. 2020;117:20538-20548.
62. Yang Y, Lian S, Meng L, Qu L, Shou C. Antibody array revealed PRL-3 affects protein phosphorylation and cytokine secretion. *PLoS One*. 2017;12:e0169665.
63. Kozlov G, Funato Y, Chen YS, et al. PRL3 pseudophosphatase activity is necessary and sufficient to promote metastatic growth. *J Biol Chem*. 2020;295(33):11682-11692.
64. Yang Y, Lian S, Meng L, et al. Knockdown of PRL-3 increases mitochondrial superoxide anion production through transcriptional regulation of RAP1. *Cancer Manag Res*. 2018;10:5071-5081.

SUPPORTING INFORMATION

Additional Supporting Information may be found online in the Supporting Information section.

How to cite this article: Abdollahi P, Vandsemb EN, Elsaadi S, et al. Phosphatase of regenerating liver-3 regulates cancer cell metabolism in multiple myeloma. *The FASEB Journal*. 2021;35:e21344. https://doi.org/10.1096/fj.202001920RR